

実験報告書様式(一般利用課題・成果公開利用)

(※本報告書は英語で記述してください。ただし、産業利用課題として採択されている方は日本語で記述していただいても結構です。)

 <p>Experimental Report</p>	承認日 Date of Approval 2014/8/18 承認者 Approver Takashi Ohhara 提出日 Date of Report 2014/8/13
課題番号 Project No. 2014A0070 実験課題名 Title of experiment Time-of-flight 3D neutron diffraction for multigrain crystallography 実験責任者名 Name of principal investigator Soeren Schmidt 所属 Affiliation Technical University of Denmark	装置責任者 Name of Instrument scientist Takashi Ohhara 装置名 Name of Instrument/(BL No.) SENJU (BL18) 実施日 Date of Experiment May 21 - June 3, 2014

試料、実験方法、利用の結果得られた主なデータ、考察、結論等を、記述して下さい。(適宜、図表添付のこと)
 Please report your samples, experimental method and results, discussion and conclusions. Please add figures and tables for better explanation.

1. 試料 Name of sample(s) and chemical formula, or compositions including physical form.
These are the samples investigated during the experiment: <ol style="list-style-type: none"> 1. Iron rods (100% Fe) with a diameter of 5 and 10 mm; 2. Nickel-Titanium (Nitinol) rods, 10 mm diameter; 3. A Bismuth (Bi) rod, 10 mm diameter; 4. Ni-superalloy rods, diameter around 2 mm; 5. Tungsten (W) pseudocubes, side of about 5 mm.

2. 実験方法及び結果 (実験がうまくいかなかった場合、その理由を記述してください。) Experimental method and results. If you failed to conduct experiment as planned, please describe reasons.
--

Experimental method. 3D neutron Diffraction (3DND) is a novel technique that uses neutrons to study the structure of polycrystalline materials, such as metals and rocks, in three dimensions. The technique is based on 3D X-ray Diffraction [1] and returns a 3D map showing position and orientation of the grains composing the considered sample.

The 3DND experiment performed at the SENJU beamline was the first of its kind, combining the use of a time-of-flight beam with the simultaneous acquisition of transmission and diffraction information via a combination of near- and far-field detectors.

Information in direct and orientation space were simultaneously recorded using, respectively, an event counting detector, later called *near-field detector*, and the diffraction detector banks of the beamline, later called *far-field detector* [2,3]. The sample was placed on a rotation stage at the centre of the diffraction detector banks, with the near-field detector a few centimetres downstream. See Fig.1 for a sketch of the detectors arrangement.

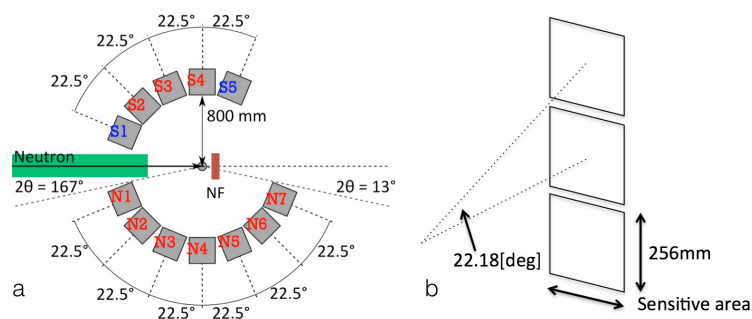


Figure 1. a: Overview of the detector setup used at BL18, J-PARC. It combined 36 scintillator detectors (far-field detectors, named S1...S5 and N1...N7) and an MPC one (near-field detector, noted as NF in the figure). The near-field detector has an active area of $28 \times 28 \text{ mm}^2$ and pixel size of $55 \mu\text{m}$. The far-field detectors consist of 12 modules made of three detectors each, arranged as shown in **b**. Each module composing the far-field detector has a size of $256 \times 256 \text{ mm}^2$, with a pixel size of 4 mm . Modified figure from [2].

Most of the beamtime was spent imaging Iron, Bismuth or Nickel samples at a number of different projections, evenly spaced across 180 or 360 degrees. A number of test measurements have also been performed to study the Tungsten and Nitinol rods: these materials require longer exposure times and have been imaged for several hours without rotating.

Data analysis. The data collected by the near- and far-field detectors are being analysed using a combination of ad-hoc developed and existing algorithms [4,5]. The basic idea is to derive the orientation of the grains from the diffraction pattern collected by the far-field detector, and the shape of the grains from the transmission signal collected by the near-field detector. In particular, the shape of the grains is determined using the corresponding “extinction spots”, recorded by the near-field detector when a grain with low-index reflections and high structure factor values satisfies the Bragg condition (see Fig. 2) [6].

For each grain, the association between a certain shape and orientation is done using the properties of the time-of-flight beam, where neutrons with different energies illuminate the sample at different times. To test the data analysis procedure, McStas Monte Carlo simulations are also being used [7].

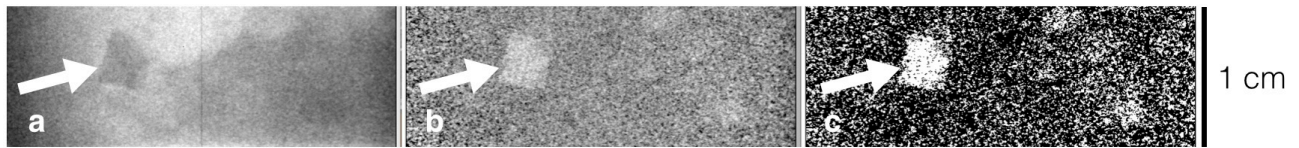


Figure 2. Different steps of the analysis procedure for the transmission data collected by the near-field detector: (a) raw data, (b) data cleaned for the open beam, (c) a threshold cut is applied to the cleaned dataset and the result is then binarised. The arrow points to an extinction spot. Sample considered: Armco Iron rod with 1cm diameter.

Results. During the experiment at BL18, we imaged 10 samples and collected tomographic data for 4 of them. Typical transmission and diffraction data are shown in Fig. 3. For the grain map, we estimate a resolution similar to what typically achieved with 3D X-ray diffraction [1].

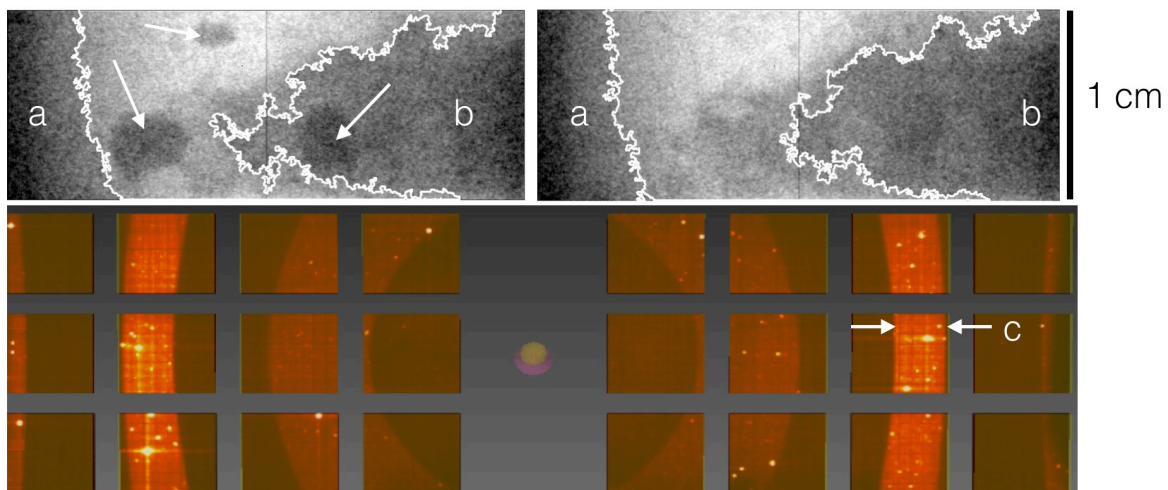


Figure 3. Typical transmission and diffraction signal recorded while imaging an Iron cylinder at the beamline BL18, J-PARC. The transmission signal (*above*), collected by the near-field detector, is shown before being processed. In the first frame (*left*) the dark spots, pointed by arrows, are the extinction spots, recorded when a grain satisfies the Bragg condition. Regions marked by (a) and (b) consist of small grains showing powder-like behavior and are also visible in the second frame, collected about 0.015\AA later. The diffraction signal collected by the far-field detectors (*below*) is visualized using STARGazerP [3]. The size of the diffraction spots on the far-field detector is proportional to the volume of the corresponding grain. The rings (c) are due to small, possibly deformed grain showing a powder-like behavior, located in regions like (a) and (b).

References

- [1] Poulsen, H.F. *et al.*, (2001). *Journal of Applied Crystallography*, 34, 751-756. [2] Tamura, I. *et al.*, (2012). *J. Phys.: Conf. Ser.* **340**, 012040. [3] Tremsin, A.S. *et al.*, (2012). *Strain*, **48**, 296-305. [4] Ohhara, T. *et al.* (2009). *Nuclear Instruments and Methods in Physics Research Section A*, **600**, 195-197. [5] Schmidt